DOI: 10.30511/pcdp.2025.2064166.1033 - ISSN: 3060-8376 - Vol 2(3), 2025

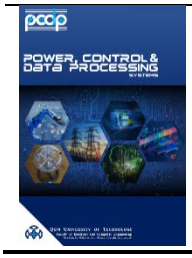

POWER, CONTROL AND DATA PROCESSING SYSTEMS

Available Online at: https://pcdp.qut.ac.ir/

Improved Robust Frequency Control Strategy in RES-Based Microgrids Using Virtual Inertia and RPCD Approach

ARTICLE INFO

Article Type
Original Research

Authors
Sajad Golshaeian[1, *]
Mahdi Najafi[1]
Gevork. B. Gharehpetian[1]
Seyed Hossein Hosseinian[1]

[1] Department of Electrical Engineering, Amirkabir University of Technology, Tehran, Iran
sajadgolshaeian@aut.ac.ir
mahdi.najafi@aut.ac.ir
grptian@aut.ac.ir
hosseinian@aut.ac.ir

**** Correspondence***
Address: Department of Electrical Engineering, Amirkabir University of Technology, Tehran, Iran.
Phone: -
Fax: -
sajadgolshaeian@aut.ac.ir

Article History
Received: June 25, 2025
Accepted: July 05, 2025
ePublished: September 01, 2025

ABSTRACT

In modern microgrid systems, maintaining frequency stability in the presence of renewable energy sources remains a critical challenge. This paper presents a resilient frequency control strategy that incorporates virtual inertia to mitigate instability issues arising from the fluctuations of renewable generation. The proposed method is based on the Robust Polynomial-Based Control Design (RPCD), which is tailored for microgrid applications to handle inherent system uncertainties. In addition, the H∞ control method is utilized as a benchmark to evaluate system performance under disturbances. The study considers distributed generation from solar and wind sources and analyzes the system's dynamic behavior in both grid-connected and islanded operating modes. In the islanded scenario—triggered by events such as voltage drops or frequency mismatches—the performance of the developed RPCD-based scheme in preserving system frequency is thoroughly evaluated. Furthermore, to investigate potential enhancements in local control performance, a version of the system with optimized PID parameters using the Shuffled Frog Leaping Algorithm (SFLA) is also examined. The results confirm that the proposed controller, with and without optimization, successfully ensures system stability under diverse and challenging operational conditions.

Keywords: Microgrids, Resilient Frequency Control, Virtual Inertia, RPCD-based controller, SFLA Optimization.

1 Introduction

Incorporating renewable energy sources like photovoltaic (PV) systems and wind turbines has significantly transformed modern power systems. While these resources contribute to reducing carbon emissions and advancing sustainable energy goals, they simultaneously reduce system inertia, creating challenges in maintaining stability and frequency regulation. Hybrid microgrids, where distributed energy resources (DERs) and energy storage systems interact dynamically, are particularly affected. Ensuring frequency stability under various conditions, such as grid-connected and islanded modes, has thus become a critical concern, highlighting the need for advanced and resilient control strategies [1].

Hybrid microgrids, which integrate distributed energy sources and storage technologies, are emerging as reliable solutions for improving energy flexibility and stability. However, the dominance of inverters in these systems means traditional inertia provided by synchronous generators is absent. Virtual inertia, implemented using grid-forming and grid-following inverters, has been proposed to address this issue. Although grid-following inverters are widely adopted due to their seamless synchronization with existing grids, they often struggle to maintain system stability, particularly during islanding scenarios [2], [3]. This underscores the necessity of developing robust frequency control mechanisms that can adapt to varying conditions and disturbances.

Advanced control techniques such as $H\infty$ and Robust Polynomial-Based Control Design (RPCD) have demonstrated their ability to manage uncertainty and ensure system performance under fluctuating conditions [4]. These approaches are particularly effective in systems with renewable energy sources, where generation variability introduces stochastic behavior and uncertainty. By integrating virtual inertia into robust control strategies, it is possible to enhance the stability and reliability of hybrid microgrids, even under challenging operational conditions [5].

This research focuses on designing a resilient virtual frequency control system based on RPCD, incorporating virtual inertia. The proposed strategy will be tested against scenarios involving high uncertainty due to renewable energy fluctuations. Initially, the microgrid's frequency behavior without virtual inertia will be evaluated to establish the need for advanced controls. Next, the $H\infty$ approach will serve as a benchmark for comparison, followed by implementing the proposed robust control system. Particular attention will be given to scenarios where the microgrid operates in islanded mode after disconnecting from the main grid due to voltage drops or frequency mismatches. The study will examine whether the proposed system can maintain microgrid stability and reliable operation under such conditions.

In light of the increasing penetration of renewable energy, one of the primary challenges faced by power systems is the inherent volatility and unpredictability of such sources [6]. Solar and wind power generation are highly dependent on weather conditions, leading to substantial fluctuations in the amount of energy produced. These fluctuations can severely impact system frequency, particularly in islanded or weakly connected microgrids, where the lack of synchronous generators exacerbates the situation [7], [8], [9]. Virtual inertia from grid-forming inverters is vital for frequency control and stability [10].

Another key challenge in microgrid operations, especially in islanded mode, is ensuring that the system can autonomously maintain its stability and respond to external disturbances. Traditional frequency control mechanisms often rely on large, centrally controlled generators that can adjust output in response to load changes. However, in microgrids with distributed generation, such as those using PV and wind systems, conventional methods may not be effective [11]. This highlights the importance of decentralized control strategies that are capable of dynamically adjusting to changes in generation and load while maintaining stable operation. The combination of virtual inertia and robust control methodologies can enable microgrids to handle disturbances more effectively, providing a more resilient and adaptive system.

Incorporating advanced control strategies into microgrid design not only enhances stability but also contributes to the broader goal of achieving a reliable and sustainable energy infrastructure. As power systems become more decentralized and diverse, the need for adaptive, resilient, and efficient control systems becomes increasingly important [12]. The RPCD approach offers a promising solution, as it allows for the integration of multiple control objectives, including frequency regulation, voltage stabilization, and power quality. By optimizing control parameters to account for system uncertainties, this method ensures that the microgrid can adapt to both expected and unexpected challenges, ensuring reliable operation even under the most demanding conditions.

Recent studies have explored various optimization techniques and control approaches to address the challenges associated with renewable energy integration in smart microgrids [13], [14]. For instance, in [15], the Shuffled Frog Leaping Algorithm (SFLA) was employed to manage DERs and implement Demand Response Programs (DRPs), with the aim of simultaneously optimizing technical, economic, and environmental objectives of smart microgrids. This approach effectively handled uncertainties in renewable energy prediction through cumulative distribution functions, and demonstrated the algorithm's capability in avoiding premature convergence and achieving global optimal solutions under various scenarios. Furthermore, in [16], SFLA was applied to enhance the performance of fuzzy-based power system stabilizers (PSS) and unified power flow controllers (UPFC), resulting in improved system damping and reduced overshoot across different operating conditions. Inspired by these applications, this study incorporates SFLA to optimize local PID controller parameters alongside the proposed RPCD-based frequency control framework. This hybrid approach aims to improve transient performance while maintaining

robust frequency regulation under high uncertainty and variable operational conditions.

In this paper, Section II will first review the presented microgrid and frequency control system. Section III will address the formulation and the proposed methods. In Section IV, the results extracted from the simulations will be discussed, and finally, the conclusion will be presented in the last section.

2 Methodology

A hybrid microgrid, in which various energy sources and loads are integrated, is shown in Figure 1. At the core of the system, a thermal power plant serves as the primary frequency control reference. This power plant plays a crucial role in maintaining grid frequency stability by adjusting its power generation. Additionally, an energy storage system, functioning as virtual inertia, is placed alongside the thermal power plant to enhance system performance and contribute to stability in response to energy fluctuations.

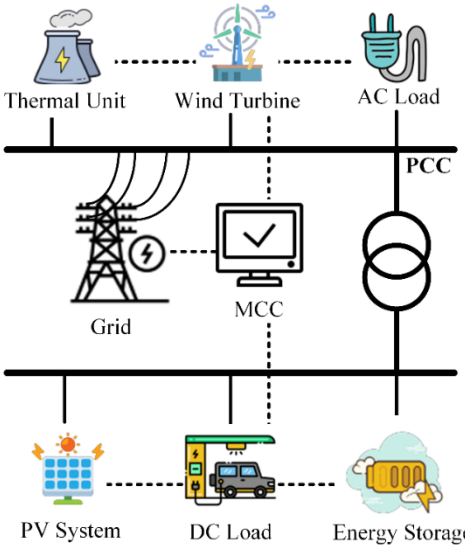

Figure 1: A case of a studied microgrid

The microgrid also includes solar and wind power plants, with the energy produced by these renewable sources being injected into the system. These renewable energy sources work in tandem with the thermal power plant and the energy storage system to ensure a reliable power supply under various conditions. All units of the microgrid are controlled by the Microgrid Central Controller (MCC). Both DC and AC loads are present in this microgrid, consuming the energy generated by these sources to meet different system demands. The microgrid is operating in grid-connected mode, where the different energy sources cooperate to maintain system stability and power quality.

Figure 2 illustrates a simplified model of the frequency control system for the studied microgrid, which also considers grid connection. For brevity, the models of the solar and wind systems are omitted in this figure. However, all parameters used in the simulations are provided in Table 1 for better understanding.

Table 1: parameters related to the proposed frequency control system

Parameter Name	Notation	Value
Governor Time Constant [s]	T_g	0.1
Turbine Time Constant [s]	T_t	0.5
Solar System Time Constant [s]	T_s	1.8
Wind Turbine Time Constant [s]	T_w	1.5
Microgrid Damping Coefficient [p.u.MW/Hz]	D	0.015
Inertia Constant [p.u.MW s]	H	0.1
Speed Droop [Hz/p.u.MW]	R	2.5
Integral Gain	K_I	0.5
Virtual Inertia (VI) Gain	K_{VI}	0.1
Virtual Inertia (VI) Time Constant [s]	T_{VI}	5
Nominal Frequency of Microgrid [Hz]	f	50

As shown in Figure 2, the microgrid receives the necessary parameters from the grid and adjusts its settings accordingly to ensure stable operation. In the following sections, various scenarios will be explored to evaluate the performance of the RPCD control algorithm and compare it with the other mentioned methods under different operating conditions. This model employs a time-varying load, and to approximate real conditions, the inputs to the models of the solar system and wind power plant are designed with uncertainties. These uncertainties are introduced to assess their impact on the dynamic behavior and stability of the system during simulations.

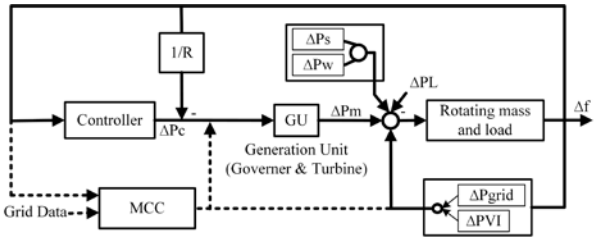

Figure 2: Simplified Model of the Frequency Control System for the Hybrid Microgrid Considering Grid Connection

The parameters related to the proposed frequency control system, including those utilized in the simulation of the hybrid microgrid, are presented in Table 1. These parameters encompass the characteristics of the thermal power plant, the virtual inertia provided by the energy storage system, the solar and wind systems, and others. This detailed set of parameters forms the foundation for analyzing the performance of the RPCD control algorithm under various scenarios discussed in the following sections [17].

3 Mathematical Formulation

3.1 Dynamic Modeling of Microgrid

In the context of frequency control, standard models for steam turbines, governors, and solar and wind systems are commonly

employed. The transfer functions of these models are defined using well-documented and recognized linear approximations. These models, developed based on experimental data and linearization around different operating points, serve as essential tools for analyzing the dynamics of power systems. The accuracy and efficiency of these models play a crucial role in ensuring the stability and reliability of the power grid under various conditions. Furthermore, they provide a foundation for designing advanced control strategies to address emerging challenges in modern power systems [18]. Equations (1) to (4) describe these models, while (5) examines the frequency deviation caused, as illustrated in the provided control diagram for frequency management.

$$\Delta P_m = \frac{1}{1+ST_t}(\Delta P_{gov}) \tag{1}$$

$$\Delta P_{gov} = \frac{1}{1+ST_g}(\Delta P_c - \frac{1}{R}\Delta f) \tag{2}$$

$$\Delta P_W = \frac{1}{1+ST_W}(\Delta P_{Wind}) \tag{3}$$

$$\Delta P_s = \frac{1}{1+ST_W}(\Delta P_{PV}) \tag{4}$$

$$\Delta f = \frac{1}{2HS+D}(\Delta P_s + \Delta P_w + \Delta P_{VI} + \Delta P_m + \Delta P_{grid} - \Delta P_L) \tag{5}$$

3.2 RPCD-based Control for Virtual Inertia

It is initially mentioned that a battery energy storage system is utilized to provide virtual inertia in the microgrid under study. In the control algorithm RPCD applied for this, a polynomial corresponding to the single-input single-output system, as presented in (6), is first considered [19].

In the proposed control system, if D is considered as the external disturbance and I as the input to the controller, the (7) will be obtained.

$$G(s) = \frac{N(s)}{D(s)} = \frac{\sum_{i=0}^{m} a_i s^i}{\sum_{i=0}^{n} b_i s^i} \tag{6}$$

$$y = \frac{N(s)F(s)}{P(s)} I + \frac{A(s)N(s)}{P(s)} D \tag{7}$$

The output y of the system under study, after considering the controller, is given. The polynomial P(s) is also defined as shown in (8).

$$P(s) = A(s)D(s) + B(s)N(s) \tag{8}$$

The numerator and denominator polynomials are also formulated similarly to the G(s). By substituting them into (8), (9) is obtained. It should be noted that for the proper operation of the controller, the condition $j \geq k$ must be satisfied.

$$P(s) = \sum_{i=0}^{j} l_i s^i D(s) + \sum_{i=0}^{k} c_i s^i N(s) \tag{9}$$

To calculate the stability indices and time constants, (10) and (11) are introduced. In (10), the stability index of the closed-loop system is defined, and in (11), the equivalent time constant of the system, which determines the system's response speed, is introduced [20].

$$\gamma_i = \frac{{a_i}^2}{(a_{i+i})(a_{i-1})} \forall i \in 1, n-1 \tag{10}$$

$$\tau = \frac{a_1}{a_0} \tag{11}$$

In this paper, the coefficients *ai* represent the coefficients of the characteristic polynomial *P*(*s*). These coefficients are used to calculate stability indices *γi*, and equivalent time constants *τ*, which are essential for designing the RPCD controller.

Using the Manabe's standard [20], the stability indices *γi*and equivalent time constant *τ*, were determined for the design of the RPCD controller. The Manabe's standard provides a systematic approach for selecting these parameters, ensuring system stability and desired dynamic performance.

According to (10) and (11), for the polynomial formed in (9), the following relation can be defined as equivalent to *P*(*s*), referred to as *Pt*(*s*):

$$P_t(s) = a_0 \left[\left\{ \sum_{i=2}^{n} \left(\prod_{j=1}^{i-1} \frac{1}{\gamma^j{}_{i-j}} \right) (\tau s)^i \right\} + \tau s + 1 \right] \tag{12}$$

To evaluate the stability of the proposed method, the Routh-Hurwitz criterion is used [21]. According to this criterion, as per (13), the following is obtained:

$$a_2 > (a_1/a_3)a_4 + (a_3/a_1)a_0$$
$$\gamma_2 > \frac{1}{\gamma_1} + \frac{1}{\gamma_3} \tag{13}$$

In this method, first, the polynomials N(s) and D(s) related to the presented model are extracted. Then, the polynomials A(s) and B(s) are defined, and by using the values of γ_i and α_i, the coefficients l_i and c_i are obtained through the comparison of P_t(s) and *P*(s). Finally, by evaluating the stability criterion, the stability of the designed controller is reviewed.

As stated in the referenced studies, the coefficients γ are determined by assuming α0=1 and τ=1.86, as shown in (14).

$$\gamma_i = [1.927, 1.39, 0.431, 0.792, 1.46]; \tag{14}$$

Based on the coefficients provided for $P_t(s)$, (15) is derived.

$$P_t(s) = 0.7s^6 + 12.1s^5 + 59.9s^4 + 249.4 \times 10^3 s^3 + 24.9 \times 10^3 s^2 + 258 \times 10^3 s + 1 \tag{15}$$

Finally, based on (9) and its expansion using N(s) and D(s) derived from the proposed model, (16) is obtained through selecting $l_0 = 0.1$, and comparing $P_t(s)$, and $P(s)$, for A(s) and B(s).

$$A(s) = 0.7s^2 + 3.5s + 0.1$$
$$B(s) = 1.125 \times 10^3 s^2 + 15.463 \times 10^3 s + 71.33 \times 10^3 \tag{16}$$

It has been verified that the stability condition defined for the proposed controller design is fully satisfied. The results pertaining to this matter will be discussed in detail in the next section.

4 Simulation Results

In this section, simulations related to the previous section will be conducted using MATLAB/Simulink. The proposed RPCD controller, derived based on the polynomials in (17), will be analyzed in detail.

Additionally, the proposed RPCD controller will be compared with the robust H∞ controller to evaluate the effectiveness of the designed approach. It is worth mentioning that the robust $H\infty$ controller and its coefficients have been obtained based on [22].

4.1 Comparative Analysis of Control Strategies in Four Operational Cases

In this study, four different scenarios are defined to analyze the performance and stability of the proposed frequency control system within the hybrid microgrid. It is assumed that the upstream grid provides a base load of 0.3 p.u to the microgrid, and at t=50, the microgrid is disconnected from the grid and will continue to operate in islanded mode.

4.1.1 First Scenario

The first scenario involves applying a step load of 0.1 p.u to the microgrid system at t=1, which is designed to examine the frequency stability and the system's response to sudden changes in load. This scenario will help assess how well the system can maintain its frequency within acceptable limits under the given load disturbance. The results of Scenario 1 are shown in Figure 3. In this scenario, no uncertainty is introduced into the system by the distributed generation sources, including solar and wind power.

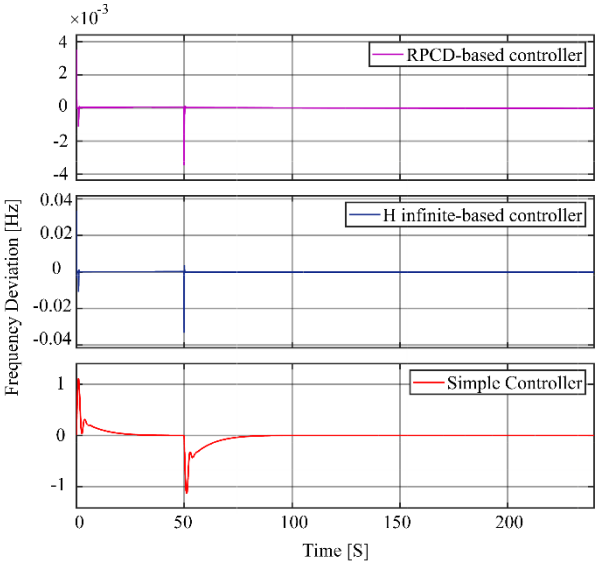

Figure 3: Frequency Response to a Step Load in Scenario

In the Figure 3, it is observed that the scenarios under investigation examine three control strategies: the simple controller, the virtual inertia controller utilizing $H\infty$, and the proposed robust RPCD controller. As observed, the frequency deviation is within the range of ±1.2 Hz for the simple controller, ±0.38 Hz for the $H\infty$ controller, and ±0.0035 Hz for the RPCD algorithm.

To preserve the stability conditions imposed by the RPCD framework while introducing some flexibility to account for system nonlinearities and uncertainties, the stability indices γi were modified based on (17), where each γi was perturbed using a small random factor δi. This ensures that all γi values remain within a reasonable range around the original Manabe's recommendations.

$$\gamma_{set,i} = \gamma_{set,base} \cdot (\delta_i + 1); i \in [2,4] \quad (17)$$

This modification ensured that the derived coefficients still satisfy the sufficient stability condition, while improving the robustness of the transient response in the presence of high RES penetration and model uncertainties. The effectiveness of this approach can be clearly observed in Figure 4, where the system response remains stable and well-damped across all gamma sets.

As illustrated in Figure 4, the proposed γi values—designed within the range defined by Manabe—yield the best performance in terms of settling time and overshoot, particularly in Scenario 1, where the time window after 50 seconds was specifically analyzed to highlight the transient behavior.

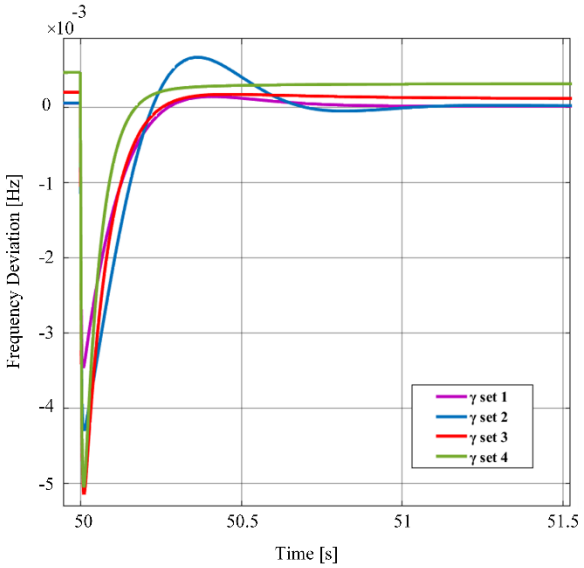

Figure 4: Comparison of transient frequency responses for various γi profiles (Scenario 1)

Compared to other tested γi sets, the proposed configuration leads to faster damping of oscillations, reduced peak deviations, and quicker convergence to the steady state. This indicates that selecting γi values close to the standard profile, while allowing slight controlled variations, can effectively enhance the system's dynamic response under high RES penetration without compromising stability.

4.1.2 Second Scenario

In Scenario 2, a variable load is connected to the microgrid to evaluate its performance under realistic and dynamic operating conditions. This scenario aims to test the adaptability and robustness of the implemented controllers when subjected to fluctuating power demands. These fluctuations, which frequently occur in practical, introduce dynamic challenges

that conventional controllers may struggle to address effectively. The time-varying load profile, depicted in Figure 5, represents practical operational scenarios.

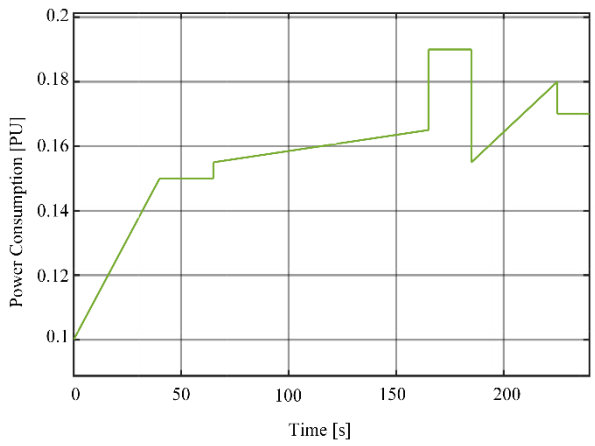

Figure 5: Time-Varying Load Profile

By analyzing the system's response under these conditions, the effectiveness of the proposed controllers in maintaining frequency stability, minimizing transient deviations, and ensuring smooth power sharing can be thoroughly assessed. This scenario helps to reveal the controllers' ability to handle realistic fluctuations, which are common in actual grid operations, thereby validating their robustness, adaptability, and suitability for deployment in modern smart microgrid environments.

According to Figure 5 and the variable load input over time, it is observed in Figure 6 that the system maintains its stability under these conditions. In this scenario, uncertainty related to solar and wind power sources is also not considered.

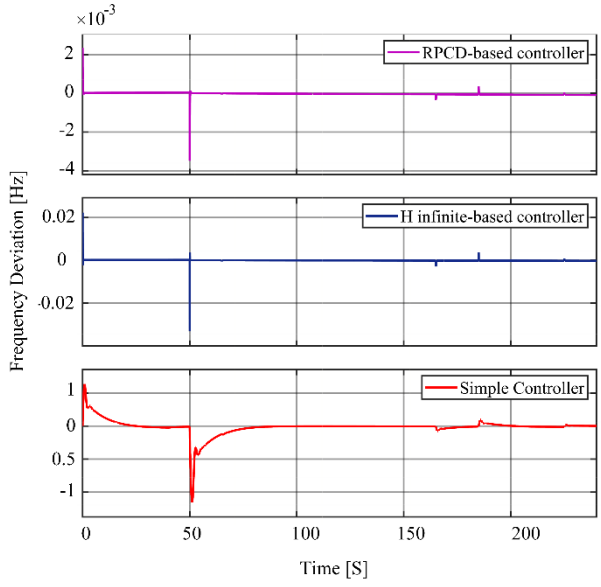

Figure 6: Frequency Response Under Time-Varying Load in Scenario 2

In Scenario 2, it is also observed that the proposed robust RPCD controller effectively maintains frequency deviations within the range of ±0.0023, outperforming the other two methods.

4.1.3 Third Scenario

The impact of uncertainty becomes particularly important when there is a high penetration of solar and wind power systems in the grid. To simulate this, a random curve will be used as the input power profile for the distributed generation sources as shown in Figure 7.

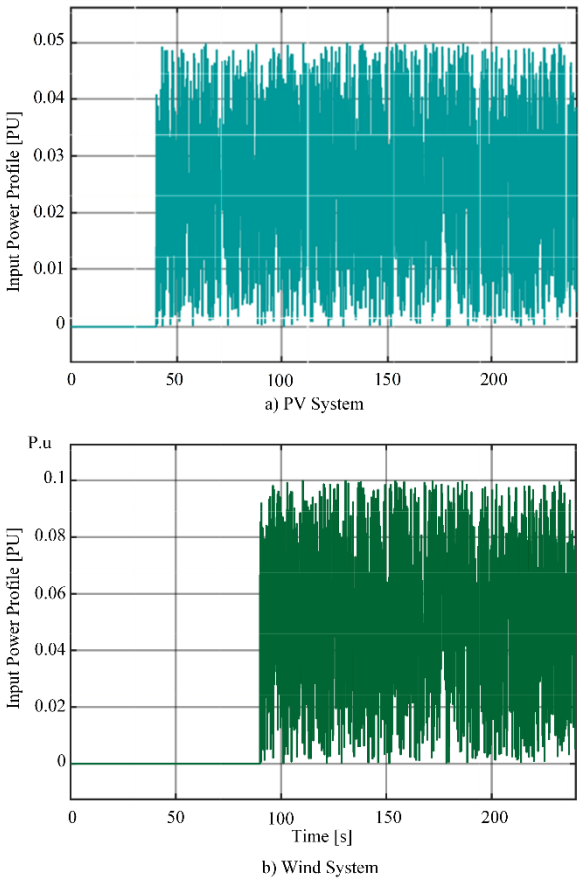

Figure 7: Input Profiles of Wind and Solar Generation

By incorporating this uncertainty into the system, the performance of the proposed controllers will be thoroughly analyzed under more realistic and dynamic conditions, highlighting their ability to maintain system stability despite fluctuations in renewable energy generation.

The wind generation is introduced at t=90s and the solar system at t=40s, adding further complexity and dynamic variation to the system. This will allow a more comprehensive evaluation of the controllers' performance under fluctuating renewable energy sources. In Figure 7, the input profiles of wind and solar generation are shown.

As shown in Figure 8, frequency deviations are effectively mitigated by the proposed controllers. Initially, a step load disturbance of 0.1 per unit is applied to the microgrid at t=0t = 0t=0, introducing a sudden imbalance between generation and

demand. Despite this abrupt change, the controllers successfully regulate the frequency and drive the system back toward its nominal value with minimal overshoot and acceptable settling time. This demonstrates the controller's capability to promptly counteract disturbances and maintain frequency stability under islanded operating conditions.

Among the controllers, the RPCD controller demonstrates superior stability and faster response compared to the others, making it more effective in handling fluctuations caused by the integration of renewable energy sources. This performance confirms the controller's capability to maintain system stability under varying conditions, including sudden load changes and the uncertainties introduced by renewable energy sources.

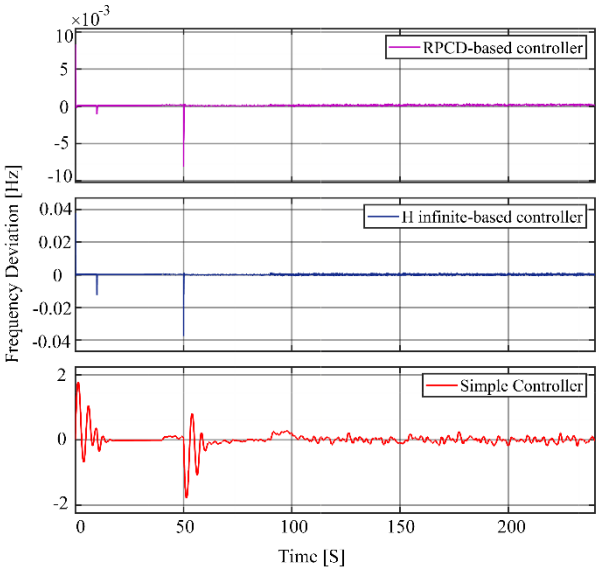

Figure 8: Frequency Response Under Renewable Energy Integration in Scenario 3

4.1.4 Fourth Scenario

In the final scenario, which combines aspects of the previous cases, the microgrid and the implemented controllers are tested under uncertain conditions and a time-varying load to evaluate their robustness and dynamic performance, as shown in Figure 9. This will allow us to assess the performance of the defined controllers under these conditions as well.

In this case, we also observe the quick and stable response of the RPCD controller, which results in a frequency deviation of ±0.00241 Hz. The frequency control operation with the *H*∞ controller shows a frequency deviation of ±0.02 Hz, while the conventional control method displays a deviation of ±1.86 Hz in its frequency control operation under these conditions.

Based on the comparative results presented in Table 2, the proposed RPCD controller demonstrates superior performance in terms of both dynamic response and frequency stability under all tested scenarios. It consistently maintains the frequency deviation within minimal bounds typically, less than ±0.004 Hz—despite disturbances and system uncertainties, especially during microgrid islanding and renewable energy fluctuation.

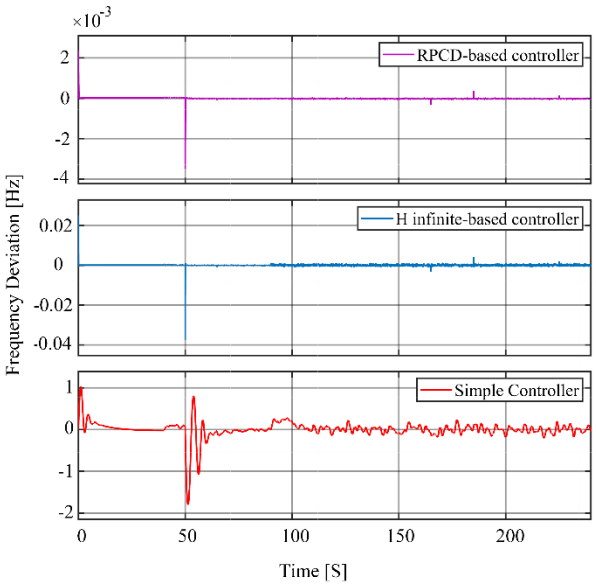

Figure 9: Microgrid Frequency Response in the Scenario 4

Compared to the simple and H∞ controllers, the RPCD strategy yields significantly lower peak frequency deviations and faster settling times. In scenarios involving high uncertainty and operational stress, such as Scenarios 3 and 4, the RPCD controller effectively limits the frequency oscillations and stabilizes the system in a timely manner, highlighting its ability to enhance resilience in hybrid microgrids.

Table 2: Comparative dynamic performance of the three controllers under all scenarios

Scenario	Controller	Settling Time (s)	Maximum Frequency Deviation (Hz)	Peak Time (s)
1	Simple	55.63	±1.1526	51.17
	H∞	50.20	±0.0335	0.035
	RPCD	50.62	±0.0035	0.0088
2	Simple	78.79	±1.1519	51.17
	H∞	50.20	±0.0333	50.04
	RPCD	50.65	±0.0035	50.01
3	Simple	98.52	±1.7932	51.36
	H∞	99.93	±0.0376	0.026
	RPCD	99.91	±0.0083	0.0065
4	Simple	98.52	±1.7984	51.36
	H∞	99.93	±0.0375	50.03
	RPCD	65.03	±0.0035	50.01

Moreover, while the H∞ controller provides acceptable improvements over the simple method in terms of reduced overshoot and moderate settling time, it still lags behind the RPCD approach in overall performance. Particularly in the critical early seconds following disturbances, the RPCD controller responds rapidly, preventing excessive overshoot and ensuring smoother frequency regulation. These observations underscore the effectiveness of the RPCD-based control strategy in maintaining frequency stability, particularly when virtual inertia is incorporated. As a result, the proposed

method offers a promising and practical solution for improving microgrid resilience under varying operational conditions.

4.2 Optimization of Local Controller Parameters Using SFLA

To further enhance the dynamic performance and robustness of the local frequency controller, the Shuffled Frog Leaping Algorithm (SFLA) was employed to optimize the controller's parameters. Unlike manually tuned or trial-and-error methods, SFLA offers a population-based metaheuristic approach that can effectively handle the nonlinearity and uncertainty inherent in hybrid microgrid systems. To identify the optimal parameters of the local controller within the proposed RPCD-based framework, the optimization problem was formulated using a performance-oriented objective function and a set of essential constraints. The cost function was defined based on the Integral of Time and Absolute Error (ITAE) criterion, as expressed in (18) [23], due to its effectiveness in penalizing sustained deviations over time and improving transient response.

$$J_{ITAE} = \int t|\Delta f|dt \qquad (18)$$

Furthermore, the optimization process was constrained by the following conditions to ensure closed-loop stability, physical realizability, and compliance with dynamic performance specifications:

- Bounded design variables: The control gains were restricted within predefined limits, i.e., $K_i \in [K_{i,\ min}, K_{i,\ max}]$, to reflect hardware and safety limitations.
- Stability constraint: The resulting controller had to satisfy the Routh-Hurwitz stability criterion, ensuring that all poles of the closed-loop system reside in the left-half complex plane.
- Performance constraints: The optimized system was required to meet minimum standards in terms of maximum allowable overshoot, settling time, and steady-state error, as dictated by system-level control objectives.

In this study, the optimization variables (e.g. K_i) were restricted to a feasible search space. Specifically, the lower and upper bounds for the gain values were set to [-10,5], respectively, based on practical considerations and stability requirements. These constraints are handled in such a way that the defined ITAE cost function is minimized, ensuring an optimal trade-off between stability, dynamic response, and control effort.

Figure 10 illustrates the frequency response results for all four scenarios using the SFLA-optimized RPCD controller, enabling a comparative analysis. To evaluate the impact of optimization on the RPCD controller, each of the four defined scenarios was additionally simulated using the RPCD strategy whose parameters were fine-tuned via the SFLA. The aim was to examine whether optimization could enhance transient performance or robustness under different operating conditions.

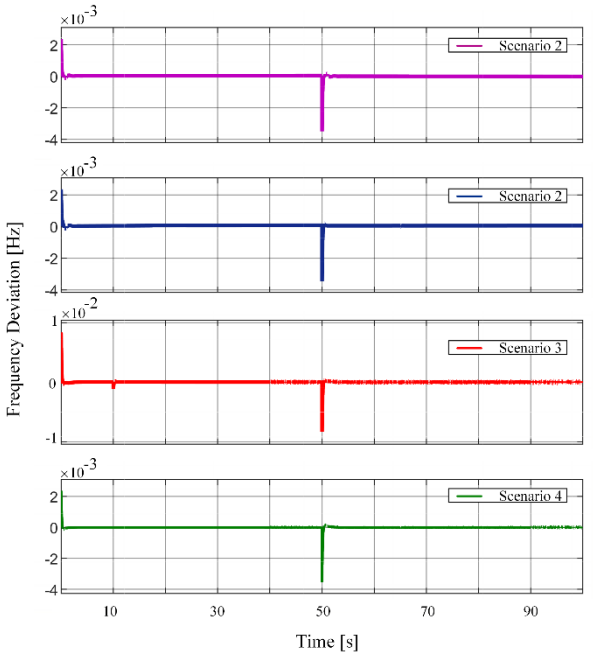

Figure 10: Frequency response of the four scenarios using the SFLA-optimized RPCD controller

Although the implementation of the SFLA algorithm for tuning the local PID controller did not significantly affect the overall settling time or steady-state peak values, it resulted in a noticeable improvement in the initial dynamic response. As shown in Table 3, the rise time decreased sharply, and both overshoot and undershoot values were significantly reduced. These observations indicate that while the RPCD controller dominates frequency stability and peak regulation, optimization of local controllers using metaheuristic algorithms like SFLA can further enhance transient performance and system responsiveness, particularly in the early moments following disturbances.

For better visualization and interpretation, the simulation time frame was uniformly considered from 0 to 100 seconds across all scenarios. On average, employing SFLA led to a 70–80% reduction in overshoot, undershoot, and rise time, while the steady-state metrics such as settling time and peak frequency deviation remained nearly unchanged.

Table 3: Evaluation of Frequency Regulation Performance of the RPCD Controller with and without SFLA Optimization

Performance Metric	Average Percentage Change Compared to Baseline (Without SFLA)
Rise Time	Decreased by approximately 78% (significant improvement in initial response)
Overshoot	Decreased by approximately 77%
Undershoot	Decreased by approximately 70%
Settling Time	Changed by less than 1% (almost no change)
Peak Value	Negligible or no change

Table 4 lists the parameters used in the Shuffled Frog-Leaping Algorithm (SFLA) for tuning the local controller. These values were selected based on practical testing and literature guidance to ensure a balance between convergence speed and performance accuracy, while also avoiding

premature convergence and maintaining adequate exploration of the search space. This careful parameter selection plays a crucial role in achieving reliable and efficient tuning outcomes.

Table 4: Configuration of the SFLA Algorithm for Local Controller Adjustment

Parameter	Value	Description
MaxIt	10	Number of global iterations
nMemeplex	4	Number of memeplex groups
nPopMemeplex	4	Number of frogs (adjusted to ≥ nVar+1)
nPop	16	Total population size
q	2	Number of parents in each memeplex
α (alpha)	5	Number of offsprings generated
β (beta)	3	Number of local iterations in FLA
σ (sigma)	1	Step size for local search
VarMin – VarMax	[–100, 1000]	Bounds for gains
nVar	3	Number of decision variables

5 Conclusion

This paper examined the frequency stability of a microgrid operating in both islanded and grid-connected modes. The microgrid system was modeled considering various influencing factors. The RPCD algorithm was then introduced, explaining how it can be used to design a resilient controller for virtual inertia, with stability conditions verified using the Routh-Hurwitz criterion. The results from the simulations showed that the RPCD-based controller outperformed both the simple and H∞-based controllers in all four defined scenarios. In addition to superior steady-state performance, the transient response of the system was further improved by optimizing the local controller parameters using the SFLA. Simulation results demonstrated that, although the settling time and steady-state frequency deviation remained largely unchanged, the use of SFLA led to a significant improvement in dynamic behavior. Specifically, overshoot, undershoot, and rise time were reduced by approximately 77%, 70%, and 78%, respectively. These enhancements resulted in a faster and smoother response to disturbances, especially in the early seconds after the system is subjected to changes. This study highlights that the RPCD-based resilient controller, particularly when fine-tuned using metaheuristic optimization, is a highly effective solution for maintaining microgrid frequency stability—even in the face of high uncertainties introduced by renewable energy sources and dynamic load variations. These findings underscore the potential of combining robust control design with optimization algorithms to enhance the performance and resilience of microgrids and sustainable power systems.

Disclosure of Potential Conflicts of Interest

The Authors declare that there is no conflict of interest

Reference

[1] S. Hasheminasab, M. Alzayed, and H. Chaoui, “A Review of Control Techniques for Inverter-Based Distributed Energy Resources Applications,” *Energies 2024, Vol. 17, Page 2940*, vol. 17, no. 12, p. 2940, Jun. 2024, doi: 10.3390/EN17122940.

[2] D. T. Rizi, M. H. Nazari, S. H. Hosseinian, M. Fani, and G. B. Gharehpetian, “Analyzing Electric Heat Pump Modeling in an Advanced Energy Hub with Renewable Energy Integration,” *2024 28th International Electrical Power Distribution Conference, EPDC 2024*, 2024, doi: 10.1109/EPDC62178.2024.10571765.

[3] R. Ahmadi, S. A. Hosseini, S. Mohammadi, R. A. Naghizadeh, and G. B. Gharehpetian, “Optimal Sizing and Sitting of Photovoltaic Distributed Generation Units Using PSO Algorithm,” *2022 12th Smart Grid Conference, SGC 2022*, 2022, doi: 10.1109/SGC58052.2022.9998913.

[4] O. Ogunbodede and T. Singh, “Differential flatness-based design of robust controllers using polynomial chaos for linear systems,” *Int J Control*, vol. 97, no. 8, pp. 1687–1703, Aug. 2024, doi: 10.1080/00207179.2023.2225661.

[5] A. Fawzy, A. Bakeer, G. Magdy, I. E. Atawi, and M. Roshdy, “Adaptive Virtual Inertia-Damping System Based on Model Predictive Control for Low-Inertia Microgrids,” *IEEE Access*, vol. 9, pp. 109718–109731, 2021, doi: 10.1109/ACCESS.2021.3101887.

[6] M. S. Alam *et al.*, “Renewable energy integration with DC microgrids: Challenges and opportunities,” *Electric Power Systems Research*, vol. 234, p. 110548, Sep. 2024, doi: 10.1016/J.EPSR.2024.110548.

[7] M. O. Qays, I. Ahmad, D. Habibi, A. Aziz, and T. Mahmoud, “System strength shortfall challenges for renewable energy-based power systems: A review,” *Renewable and Sustainable Energy Reviews*, vol. 183, p. 113447, Sep. 2023, doi: 10.1016/J.RSER.2023.113447.

[8] F. Ueckerdt, R. Brecha, and G. Luderer, “Analyzing major challenges of wind and solar variability in power systems,” *Renew Energy*, vol. 81, pp. 1–10, Sep. 2015, doi: 10.1016/J.RENENE.2015.03.002.

[9] M. Najafi, P. Sadat, M. Faraji, G. B. Gharehpetian, A. Khorsandi, and S. H. Hosseinian, “MPSO-Based Economic Optimal Design of an Isolated Industrial Microgrid Considering LPSP Concept and Covering System Uncertainties,” *2024 11th Iranian Conference on Renewable Energy and Distribution Generation, ICREDG 2024*, 2024, doi: 10.1109/ICREDG61679.2024.10607808.

[10] B. K. Poolla, D. Groß, and F. Dörfler, “Placement and Implementation of Grid-Forming and Grid-Following Virtual Inertia and Fast Frequency Response,” *IEEE Transactions on Power Systems*, vol. 34, no. 4, pp. 3035–3046, Jul. 2019, doi: 10.1109/TPWRS.2019.2892290.

[11] H. Haes Alhelou, M. E. Hamedani-Golshan, R. Zamani, E. Heydarian-Forushani, and P. Siano, “Challenges and Opportunities of Load Frequency Control in Conventional, Modern and Future Smart Power Systems: A Comprehensive Review,” *Energies 2018, Vol. 11, Page 2497*, vol. 11, no. 10, p. 2497, Sep. 2018, doi: 10.3390/EN11102497.

[12] M. U. Safder, M. J. Sanjari, A. Hamza, R. Garmabdari, M. A. Hossain, and J. Lu, “Enhancing Microgrid Stability and Energy Management: Techniques, Challenges, and Future Directions,” *Energies 2023, Vol. 16, Page 6417*, vol. 16, no. 18, p. 6417, Sep. 2023, doi: 10.3390/EN16186417.

[13] A. Khorsandi, M. A. S. Masoum and S. M. T. Bathaee, "Hybrid shuffled frog leaping algorithm and Nelder–Mead simplex search for optimal reactive power dispatch," *IET Generation, Transmission & Distribution*, vol. 5, no. 2, pp. 249–256, Feb. 2011, doi: 10.1049/iet-gtd.2010.0256.

[14] S. P. S. Shandiz, M. Najafi, and S. H. H. Sadeghi, "GA-Based Optimization of DG Sizing and Placement for Long-Term Cost-Effective Planning of Wind and Solar Energy Integration," in *Proc. 2024 14th Smart Grid Conference (SGC)*, Tehran, Iran, 2024, pp.

[15] N. Gouda and H. H. Aly, "Distributed Energy Sources Management using Shuffled Frog-Leaping Algorithm for Optimizing the Environmental and Economic Indices of Smart Microgrid," in *Proc. 2024 ASU Int. Conf. Emerging Technologies for Sustainability and Intelligent Systems (ICETSIS)*, Cairo, Egypt, 2024.

[16] M. Abedini and M. Abasi, "Optimization of PSS and UPFC Controllers to Enhance Stability by Using a Combination of Fuzzy Algorithm and Shuffled Frog Leaping Algorithm," *J. Appl. Res. Electr. Eng.*, vol. 3, no. 2, 2024.

[17] K. MASUI, S. TAKAMURA, and T. NAMERIKAWA, "Load Frequency Control of a Microgrid Based on $H\infty$ Control Considering Response Speed of Generators," *Transactions of the Society of Instrument and Control Engineers*, vol. 51, no. 8, pp. 570–578, 2015, doi: 10.9746/SICETR.51.570.

[18] M. Saeed Uz Zaman, S. B. A. Bukhari, K. M. Hazazi, Z. M. Haider, R. Haider, and C. H. Kim, "Frequency Response Analysis of a Single-Area Power System with a Modified LFC Model Considering Demand Response and Virtual Inertia," *Energies 2018, Vol. 11, Page 787*, vol. 11, no. 4, p. 787, Mar. 2018, doi: 10.3390/EN11040787.

[19] M. Heshmati, R. Noroozian, S. Jalilzadeh, and H. Shayeghi, "Optimal design of CDM controller to frequency control of a realistic power system equipped with storage devices using grasshopper optimization algorithm," *ISA Trans*, vol. 97, pp. 202–215, Feb. 2020, doi: 10.1016/J.ISATRA.2019.08.028.

[20] Bhaba. P.K and Somasundaram. S, "Real Time Implementation of A New CDM-PI Control Scheme in A Conical Tank Liquid Level Maintaining System," *Mod Appl Sci*, vol. 3, no. 5, p. p38, Apr. 2009, doi: 10.5539/MAS.V3N5P38.

[21] M. Soliman and M. N. Ali, "Parameterization of robust multi-objective PID-based automatic voltage regulators: Generalized Hurwitz approach," *International Journal of Electrical Power & Energy Systems*, vol. 133, p. 107216, Dec. 2021, doi: 10.1016/J.IJEPES.2021.107216.

[22] T. Kerdphol, F. S. Rahman, Y. Mitani, M. Watanabe, and S. Kufeoglu, "Robust Virtual Inertia Control of an Islanded Microgrid Considering High Penetration of Renewable Energy," *IEEE Access*, vol. 6, pp. 625–636, 2018, doi: 10.1109/ACCESS.2017.2773486.

[23] S. Golshaeian, M. H. Nazari and S. H. Hosseinian, "An Innovative PID Controller Optimization Algorithm for Two-area Power System Frequency Control and Monitoring," *2024 9th International Conference on Technology and Energy Management (ICTEM)*, 2024, doi: 10.1109/ICTEM60690.2024.10632027.